Anal. Chem. **2002,** *74,* 2240−2247

Particles for Multiplexed Analysis in Solution: Detection and Identification of Striped Metallic Particles Using Optical Microscopy

Ian D. Walton, Scott M. Norton, Arjuna Balasingham, Lin He, Dominador F. Oviso, Jr., Dimpy Gupta, Paul A. Raju, Michael J. Natan, and R. Griffith Freeman*

SurroMed, Inc., 2375 Garcia Avenue, Mountain View, California 94043, and Nanoplex Technologies, Inc., 2375 Garcia Avenue, Mountain View, California 94043

In this report, we present data demonstrating that cylindrical metallic particles, with various submicrometer striping patterns, may be readily distinguished in an optical microscope. Accurate particle identification is discussed relative to synthesis reproducibility and the limitations of optical microscopes. Results from a library of these particles, of which over 100 different striping patterns have been produced, are presented. For these particles, made with Au and Ag stripes, more than 70 patterns may be identified with greater than 90% accuracy. The ability to chemically modify the surface of these particles, making them useful for bioanalytical measurements, is also demonstrated. Finally, we discuss improvements in our manufacturing and identification processes that will lead to both larger numbers of striping patterns and improved identification accuracy.

The use of micrometer- and nanometer-dimensioned metal particles as elements of chemical and biochemical measurement systems has a long history and is rapidly becoming widespread. Au nanoparticles have been employed in the widest variety of measurements, most notably transmission electron microscopy (TEM)[1] and surface-enhanced Raman scattering (SERS),[2−6] but also to detect single-nucleotide sequence mismatches[7] and to amplify the signal obtained from surface plasmon resonance (SPR).[8] In addition, Au particles have been used as part of a high-throughput screening method,[9] to alter selectivity in capillary electrophoresis,[10] and in a particle-binding method where Au content was measured by anodic stripping voltammetry.[11] In these systems, the Au particles act to enable detection, but do not vary from analyte to analyte, and so do not provide directly any information on chemical identity.

An alternative approach is to use small particles as identification tags, in the same general way that fluorescent or radiolabeled molecules may be used as tags. In this approach, each particle tag has a unique identifying feature that distinguishes it from other tags. Also, each tag is chemically modified such that it will bind to, and report on, a specific chemical entity. Currently, the method of choice for the identification of these particles is fluorescence.[12,13] In addition to providing high sensitivity, the fluorescence emission spectra of the particles provide information on the identity of the particles. In particular, dye-impregnated polymer beads are being used as the basis for a variety of multiplexed biological measurements,[12] and a similar approach, using semiconductor quantum dots embedded in polymer spheres, has recently been reported.[13] Fluorescent dye-impregnated polymer beads have also been immobilized at the end of a fiber-optic probe generating a microsphere array that was used to detect 25 different oligonucleotides.[14] One problem with using fluorescence for both particle encoding and analyte quantification, as is done in the methods above, is that the spectral region used by the quantification fluorophore cannot be used for encoding, thus limiting the variety of encoded particles.

An additional and often overlooked optical characteristic of materials is their reflectivity. Recently, we described the synthesis of striped metal rods where the stripes may be decoded on the basis of the difference in reflectivity of the component metals.[15] We call these particles Nanobarcodes particles (or NBCs for short). While there are other analytical methods based on

* To whom correspondence should be addressed. E-mail: gfreeman@nanoplextech.com. Fax: (650) 230-1960.

(1) Handley, D. A. In *Colloidal Gold: Principles, Methods, and Applications*; Hayat, M. A., Ed.; Academic Press: San Diego, CA, 1989; Vol. 1, Chapter 1.
(2) Creighton, J. A.; Blatchford, C. G.; Albrecht, M. G. *J. Chem. Soc., Faraday Trans. 2* **1979**, *75*, 790−798.
(3) Freeman, R. G.; Grabar, K. C.; Allison, K. J.; Bright, R. M.; Davis, J. A.; Guthrie, A. P.; Hommer, M. B.; Jackson, M. A.; Smith, P. C.; Walter, D. G.; Natan, M. J. *Science* **1995**, *267*, 1629−1632.
(4) Lee, Y.-H.; Farquharson, S. *Proc. SPIE* **2001**, *4206*, 140−144.
(5) Olson, L. G.; Lo, Y.-S.; Beebe, T. P.; Harris, J. M. *Anal. Chem.* **2001**, *73*, 4268−4276.
(6) Kim, B.; Tripp, S. L.; Wei, A. *J. Am. Chem. Soc.* **2001**, *123*, 7955−7956.
(7) Taton, T. A.; Mirkin, C. A.; Letsinger, R. L. *Science* **2000**, *289*, 1757−1760.
(8) He, L.; Musick, M. D.; Nicewarner, S. R.; Salinas, F. G.; Benkovic, S. J.; Natan, M. J.; Keating, C. D. *J. Am. Chem. Soc.* **2000**, *122*, 9071−9077.
(9) Englebienne, P.; Van Hoonacker, A.; Verbas, M. *Analyst* **2001**, *126*, 1645−1651.
(10) Neiman, B.; Grushka, E.; Lev, O. *Anal. Chem.* **2001**, *73*, 5220−5227.
(11) Dequaire, M.; Degrand, C.; Limoges, B. *Anal. Chem.* **2000**, *72*, 5521−5528.
(12) Cortese, J. D. *Scientist* **2000**, *14*, 16.
(13) Han, M.; Gao, X.; J Su, Z.; Nie, S. *Nat. Biotechnol.* **2001**, *19*, 1−6.
(14) Ferguson, J. A., Steemers, F. J., Walt, D. R. *Anal. Chem.* **2000**, *72*, 5618−5624.
(15) Nicewarner-Peña, S. R.; Freeman, R. G.; Reiss, B. D.; He, L.; Peña, D. J.; Walton, I.; Cromer, R.; Keating, C. D.; Natan, M. J. *Science* **2001**, *293*, 137−141.

10.1021/ac020073w CCC: $22.00
Published on Web 04/17/2002

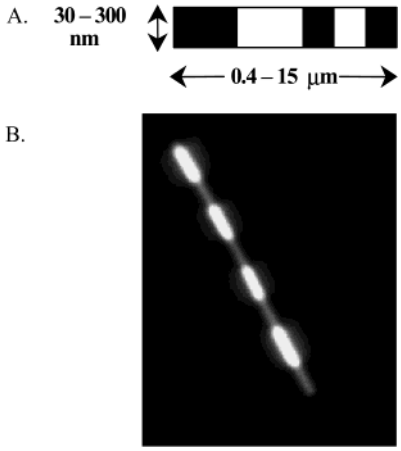

Figure 1. Nanobarcodes particles (NBC). (A) Schematic image demonstrating range of possible dimensions and one possible striping pattern. (B) Optical microscope image of a single particle. The particle contains alternating sections of Ag and Au and is 6.3 μm in length. Ag is the brighter material at this wavelength (405 nm). The apparent difference in the thickness of the Ag and Au stripes is due to the difference in brightness, not to a true difference in particle diameter.

reflectivity, including FT-IR when coupled with attenuated total reflectance, particle identification by reflectivity is rare. Surface plasmon resonance can detect the presence of Au particles near the SPR surface with great sensitivity[8] but cannot be used to distinguish between particles of similar composition and size. Our striped metal particles have tremendous potential for multiplexed assays and may be readily distinguished by optical reflectivity using a microscope. These particles are cylindrically shaped metal rods, typically 300 nm in diameter and 1−10 μm in length (Figure 1). The particles are formed by electrodeposition of alternating layers of metals (or other materials) in a preformed template.

Since the publication of early papers describing the use of templates for nanoparticle, nanostructure, and nanowire synthesis,[16−18] template-guided synthesis of anisotropic nanoparticles has been used to make and study numerous interesting materials. For example, both alumina and polycarbonate templates have been used to make electronically conductive nanostructures[19] and polymer microtubules.[20] The properties of materials embedded in or released from the templates have been studied extensively,[17,21−26] and metal microtubules embedded in the templates have been used as controllable pores for both ion transport[27] and protein separation.[28] In addition, striped metallic particles have been coated with DNA and assembled onto a lithographically defined surfaces in a first step toward using such particles in electronic devices.[29]

Table 1. Calculated Number of Available Striping Patterns for a Given Number of Metals and Equal Length Stripes[30]

no. of stripes	no. of metals			
	2	3	4	5
1	2	3	4	5
2	3	6	10	15
3	6	18	40	75
4	10	45	136	325
5	20	135	544	1625
6	36	378	2080	7875
7	72	1134	8320	39375
8	136	3321	32896	195625
9	272	9963	131584	978125
10	528	29649	524800	4884375
11	1072	88938	2099200	24421875

Table 1 illustrates the number of different barcode patterns that may be generated when various numbers of metals (different reflectivity) and different numbers of stripes (constant stripe length) are used. These values reflect the fact that our particles have no inherent orientation. The result of this is that the striping pattern AABA (where A and B represent stripes of different materials) is indistinguishable from ABAA. Even with this fact, it is theoretically possible to achieve more than 1000 different striping patterns with only two metals and 11 stripes. The addition of a third metal reduces the number of stripes needed to make 1000 patterns by almost a factor of 2. Including four metals in the striping pattern theoretically allows the production of tens to hundreds of thousands of combinations with fewer than 10 stripes.

Because it is possible to attach molecules (via chemisorption, physisorption, etc.) to the metal particle surface, and because these attached molecules can in many cases be chosen to bind specific targets, the striped particles can be turned into substrates for the capture and identification of analytes of interest. Specifically, both Au and Ag surfaces have been chemically modified in various ways. A few examples include organothiol modification of Au,[31] avidin and streptavidin on both Au and Ag,[32] β-galactosidase and choline-receptor protein on Au,[33] and antibody immobilization on Au.[34]

We have generated NBCs with more than 100 different striping patterns based on a 2-metal, 8-stripe design. This study focuses on the tools used for the detection and identification of such NBCs

(16) Penner, R. M.; Martin, C. R. *Anal. Chem.* **1987**, *59*, 2625−2630.
(17) Tierney, M. J.; Martin, C. R. *J. Phys. Chem.* **1989**, *93*, 2878−2880.
(18) Al-Mawlawi, D.; Liu, C. Z.; Moskovits, M. *J. Mater. Res.* **1994**, *9*, 1014−1018.
(19) Martin, C. R. *Acc. Chem. Res.* **1995**, *28*, 61−68.
(20) Cepak, V. M.; Martin, C. R. *Chem. Mater.* **1999**, *11*, 1363−1367.
(21) Foss, C. A.; Tierney, M. J.; Martin, C. R. *J. Phys. Chem.* **1992**, *96*, 9001−9007.
(22) Hornyak, G. L.; Patrissi, C. J.; Martin, C. R. *J. Phys. Chem. B* **1997**, *101*, 1548−1555.
(23) Al-Rawashdeh, N. A. F.; Sandrock, M. L.; Seugling, C. J.; Foss, C. A. *J. Phys. Chem. B* **1998**, *102*, 361−371.
(24) Sandrock, M. L.; Foss, C. A. *J. Phys. Chem. B* **1999**, *103*, 11398−11406
(25) Al-Mawlawi, D.; Coombs, N.; Moskovits, M. *J. Appl. Phys.* **1991**, *70*, 4421−4425.
(26) Al-Mawlawi, D.; Liu, C. Z.; Moskovits, M. *J. Mater. Res.* **1994**, *9*, 1014−1018.
(27) Nishizawa, M.; Menon, V. P.; Martin, C. R. *Science* **1995**, *268*, 700−702.
(28) Yu, S.; Lee, S. B.; Kang, M.; Martin, C. R. *Nano Lett.* **2001**, *1*, 495−498.
(29) Reiss, B. D.; Mbindyo, N. K.; Martin, B. R.; Nicewarner, S. R.; Mallouk, T. E.; Natan, M. J.; Keating, C. D. *Mater. Res. Soc. Symp. Proc.* **2001**, *635*, C6.2.1-C6.2.6.
(30) The number of combinations available where M is the number of distinct materials, n is the number of stripes, and the rod is inherently asymmetric is M^n. If rod orientation cannot be determined, then the formula becomes, total of combinations = $(M^n + M^{\mathrm{ceil}(n/2)})/2$, where ceil() is the ceiling function such that $n/2$ is rounded up.
(31) Bain, C. D.; Troughton, E. B.; Tao, Y.-T.; Evall, J.; Whitesides, G. M.; Nuzzo, R. G. *J. Am. Chem. Soc.* **1989**, *111*, 321−325.
(32) Ebersole, R. C.; Miller, J. A.; Moran, J. R.; Ward, M. D. *J. Am. Chem. Soc.* **1990**, *112*, 3239−3241.
(33) Madoz, J.; Kuznetzov, B. A.; Medrano, F. J.; Garcia, J. L.; Fernandez, V. M. *J. Am. Chem. Soc.* **1997**, *119*, 1043−1051.
(34) Karyakin, A. A.; Presnova, G. A.; Rubtsova, M. Y.; Egorov, A. M. *Anal. Chem.* **2000**, *72*, 3805−3811.

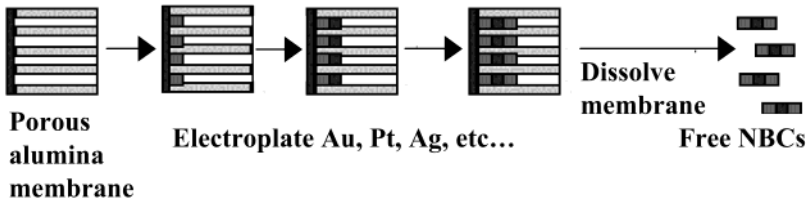

Figure 2. Schematic of NBC growth and release.

in a 2-D image. This includes the optical hardware that has been employed to generate images as well as the software that has been developed to process images. We also present data demonstrating the ability to carry out chemical measurements on these particles.

EXPERIMENTAL SECTION

NBC Synthesis. NaOH (6.0 M) and concentrated HNO_3 were obtained from VWR and 2-mercaptoethoanesulfonic acid, sodium salt (MESA) was obtained from Aldrich. Ag Plating solutions (ACR 1025 Ag Streak Bath and Silver Cy-less Solution) were obtained from Technic, and the Au plating solution (Neutronex 309 Make-Up) was obtained from Enthone. Alumina membranes (0.2-μm pore size, Anodisc) were obtained from Whatman. Dominar, Inc. carried out the evaporation of Ag onto the alumina disks.

NBC synthesis was developed based on the work of Martin and Moskovits[16−18] and performed essentially as detailed by Reiss et al.[35] Before electroplating can commence, 0.5−1.0 μm of Ag is thermally evaporated and deposited on one surface of the membrane to provide electrical contact for further electrodeposition. The membranes are placed in an electroplating system, and additional Ag is deposited to further seal the membrane (10−20 min, −6.25 mA, 1025 Ag Streak Solution) and fill the highly branched region near the surface of the templates (20 min, −1.75 mA, Silver Cy-less Solution). After that, alternating metal layers are built up as shown in Figure 2. When plating is complete, the silver backing is first dissolved with 40% HNO_3, after which, the entire membrane is placed in a 1.5-mL Eppendorf tube and the alumina pore structure is dissolved in a mixture containing 200 μL of 20 mM MESA and 1 mL of 3 M NaOH, leaving free rods. For those cases where the particles have a terminal Ag stripe, a short Au cap must be added to prevent dissolution of the Ag stripe when the Ag backing is removed. The only significant change from our procedure in ref 35 has been the substitution of cyanide-free plating solutions for those containing cyanide, which were previously used. Because the cyanide-free solutions provide higher plating efficiencies, both lower currents and shorter times may be used to produce segments of a desired length. It should be noted that the manufacture of NBCs in an eight-stripe library does not always require eight solution changes. As an example, for the pattern 00011000, Au is deposited for 36 min (3 × 12) at −1.10 mA of current. The plating solution is changed, and Ag is then deposited for 24 min (2 × 12) at −1.05 mA. Finally, the Ag solution is replaced with Au and a current of −1.10 mA is run through the cell for an additional 36 min. Only the stripe pattern 01010101 requires contact with eight different solutions during NBC creation (actually nine because of the short Au cap that deposited after the final Ag stripe).

NBC Detection. The detection system is based on a Zeiss Axiovert 100 microscope. A 175-W Xe lamp (Sutter Instruments) provides illumination. Images are acquired with a cooled CCD camera (Photometrics CoolSnapFX). The *xyz* stages (Prior) and filter wheels (Sutter Instruments) are fully automated. Fine focus is obtained with a piezoelectric drive (Polytec PI PIFOC) for the objective. Images are typically obtained with 1.4 NA 63× and 100× objectives for maximum resolution. An additional 1.6× magnifier is used to provide a total 160× enlargement from image to camera. The whole system is computer controlled (MetaMorph software from Universal Imaging). With automatic focus, this system can take a reflectance and fluorescence image pair in less than 10 s.

Image Processing. We have developed a software application for the analysis of microscope images that is designed to provide automated NBC identification and fluorescence measurements. This software also provides some additional data, such as particle position, length, and diameter. The output is a table listing each particle found and features for that particle.

The automated image processing solution for NBC images requires several critical features. It must handle multiple images, both in the sense of analyzing and coupling the reflectance (RFL) and fluorescent images (FL) and in the sense of amassing statistics from many RFL/FL pairs. It must work over a large range of image conditions and accept some degree of blurring and other aberrations in the images. The software is designed to consider only single rods. Coincident rods and large clumps are rejected since they can confound rod identification and increase the error in fluorescence quantitation. We accept a higher false negative rate (missed NBCs) in order to produce a lower false positive rate (misidentified NBCs).

Processing begins with the application of a high-pass filter to the reflectance image. This has the effect of both enhancing the edges of the rods and separating those rods that are close in proximity. Then the image noise is assessed using a peak−peak noise algorithm.[36] The image noise, combined with the median background level, is used to determine the threshold level that must be applied for segmentation, a method of isolating objects in a binary image. Applying a threshold to the image produces a binarized image whose nonzero pixels correspond to nanobars and whose zeroed pixels correspond to background.

The binarized image is analyzed to eliminate all blobs that are not single rods. Each indexed region or "blob" is first tested for size in pixels, such that blobs exceeding a certain size are discarded. The Zhang/Suen/Stentiford/Holt algorithm[37] is used to thin (skeletonize) the nanobar images. Next, thinned rods that are below a certain length threshold are discarded.

(35) Reiss, B. D.; Freeman, R. G.; Walton, I. D.; Norton, S. M.; Smith, P. C. Stonas, W. G.; Keating, C. D.; Natan, M. J. *J. Electroanal. Chem.* **2002**, *522*, 95−103.

(36) Norton, S. M.; Winkler, J.; Dietz, L. J. *Proc. SPIE* **2000**, *3921*, 20−30.

(37) Parker, J. R. *Algorithms for Image Processing and Computer Vision*; Wiley and Sons: New York, 1997.

Finally, the thinned representation of the NBC is fitted to a line using a least-squares fitting algorithm in polar coordinates. If the residual exceeds a user-defined threshold, the blob is discarded. Given that the thinning algorithm uses only the binarized blob to determine the skeleton and does not give any weight to the intensity of the pixels within the blob, a refitting line algorithm is then used to ensure that the line traverses the vibrant pixels. This algorithm identifies the pixels with the highest intensity within a short distance of the initial fit line. The least-squares fitting algorithm is then reapplied using these marked pixels.

The end points of the NBCs were refined using a dynamic threshold calculation. Initial end points were obtained from the binarized image based on the image-wide threshold. The pixel intensities at the estimated end of the particle were then averaged to give an intensity value for the terminal stripe. A percentage of this value is used as the local threshold for end point determination. The line is extended until the intensity falls below the local threshold. After the end points are determined, the previously determined best-fit line is used to extract the intensity level of the nanobar from the original bright-field image. For this paper, the maximum value within four pixels perpendicular to the best-fit line was used for the extracted line profile.

Once the line profile has been extracted from the image it is compared to a model profile for each of the possible NBC striping patterns that could be present in the image. This is done by carrying out a correlation calculation on the line profile with each possible model profile. In the present implementation, an eight-striped NBC with only two metals, such as "Ag−Au−Ag−Au−Au−Au−Ag−Ag", is represented in a simple binary fashion as 10100011. Each 1 is assigned the reflectance of Ag at the wavelength of interest, and each 0 is assigned the reflectance of Au. The 10100011 bar profile is then expanded to a preset number of pixels and convolved with a pulse wave to produce a smoother profile that more closely resembles the average extracted profile.

The model profiles and extracted profiles are stretched to a fixed length and subsequently correlated against each other. The highest correlation value represents the corresponding NBC flavor that best matches the extracted data profile.

Once a NBC has been identified, the fluorescent intensity of the NBC is assessed using the stored fluorescent image. The accepted method is to use pixels from the conjunction of a grown reflectance "blob" and the thresholded fluorescence image. A reflectance blob is grown by amassing every pixel that is adjacent to its border. The software generates mean, mode, median, and standard deviation of the background-subtracted values for the fluorescence. Finally, the correlations and intensity values are stored for each rod and the next image in the batch is analyzed.

Once all images have been analyzed, the data for NBC stripe pattern is combined to give intensity statistics for each type of NBC over many images that compose an assay well. This information is written out to a tab delimited text file and may then be analyzed using other packages to generate fluorescence statistics on populations as well as statistics on identification accuracy.

On-Particle Assay. Mercaptoundecanoic acid (MUA) and phosphate-buffered saline pellets (PBS buffer, including 0.01 M phosphate, 0.12 M NaCl, and 0.0027 M KCl) were obtained from Aldrich (Milwaukee, WI). Bovine serum albumin (BSA) was purchased from Sigma (Milwaukee, WI). NeutrAvidin, 1-ethyl-3-(3-dimethylaminopropyl) carbodiimide (EDC), and *N*-hydroxylulfosuccinimide (s-NHS) were purchased from Pierce (Rockford, IL). A biotinylated squarate dye was synthesized in-house.

Particles of flavor 00010111, 00010001, and 00011011 were incubated in a 10 mM MUA/C_2H_5OH solution overnight. Carboxyl groups on particle surfaces were activated using EDC and s-NHS reagents and then cross-linked to the amino groups in NeutrAvidin. Following the removal of proteins by extensive washes, two additional flavors of particles, 00001111 and 00010101, were mixed with NeutrAvidin-coated particles. After 30-min incubation with 1 μM biotinylated dyes in PBS/BSA buffer, the mixture of particles was rinsed with PBS/BSA buffer to remove nonspecifically bound molecules.

The previously described microscope was used to capture the reflectance and fluorescence images of dye-captured particles. A 100×, 1.4 NA objective lens, a 630-nm excitation filter with 50-nm band-pass, and a 700-nm detection filter with 75-nm band-pass were used.

RESULTS AND DISCUSSION

Figure 1B illustrates the ability to distinguish between Ag and Au in a striped particle. The particle is composed of alternating stripes of Au (less reflective) and Ag (more reflective), and the image was collected with illumination at 405 nm. SEM images have shown that the apparent difference in thickness between the Ag and Au stripes is due to the difference in brightness, not a true difference in particle diameter.

The reliable identification of striped metal particles depends on three factors: the ability to precisely and reproducibly synthesize the particles, the ability of the optical system to transfer information to the CCD, and the ability of software to find particles in a two-dimensional image. The following sections will present our findings in that order.

NBC Synthesis Variation. Figure 3A is an image of NBCs made with the 00001001 striping pattern while Figure 3B shows the line profiles for 10 of the particles in the image. The line scans were normalized to constant length as is also done in the particle identification software. For this batch of NBCs, the average length of the particles was 5.8 μm. The similarity of the particles is evident in both the microscope image and in the line scans. To be successful, the software must find as many of the NBCs as possible in the image and correctly assign them to 00001001, rather than one of the many other possibilities. The first factor that contributes to correct identification is the control of synthesis. To determine plating variability, we have measured the length of the Ag and Au stripes of a number of NBCs as well as the overall length (Table 2). The relative standard deviations for deposition of Ag are generally larger than those for the deposition of Au, and as a result, those NBCs with more Ag in them tend to identify with lower accuracy (see below). The values for both Ag and Au are better that those we previously reported.[35] We ascribe this improvement to a change to plating solutions that do not contain cyanide.

To test the accuracy of the software identification process, multiple images of a sample containing a single type of NBC were collected. In the limit of perfect NBC synthesis, perfect image collection, and perfect data analysis, all of the particles in the

Table 2. NBC Segment Measurements[a]

stripe pattern	Ag stripe(s)	Au stripe(s)	total length	ratio
00000001	0.80 ± 16%		7.32 ± 7%	0.110 (1 Ag/total)
00000100	0.77 ± 14%		5.98 ± 6%	0.127 (1 Ag/total)
00001001	0.71 ± 15%	1.34 ± 7%	5.71 ± 7%	0.124 (1 Ag/total), 0.234 (2 Au/total)
00111100	3.64 ± 13%		7.09 ± 9%	0.513 (4 Ag/total)
00110011	1.63 ± 17%	1.57 ± 9%	6.57 ± 11%	0.248 (2 Ag/total), 0.239 (2 Au/total)

[a] Relative standard deviation reported in percent. More than 100 particles were measured for each entry in the table. Underlined type indicates the stripes that were measured. The ratio measurements are the average length of the stripe divided by the average total length. In the ideal case, the value should be 0.125 (1/8) for a single stripe, 0.25 (2/8) for two stripes, etc.

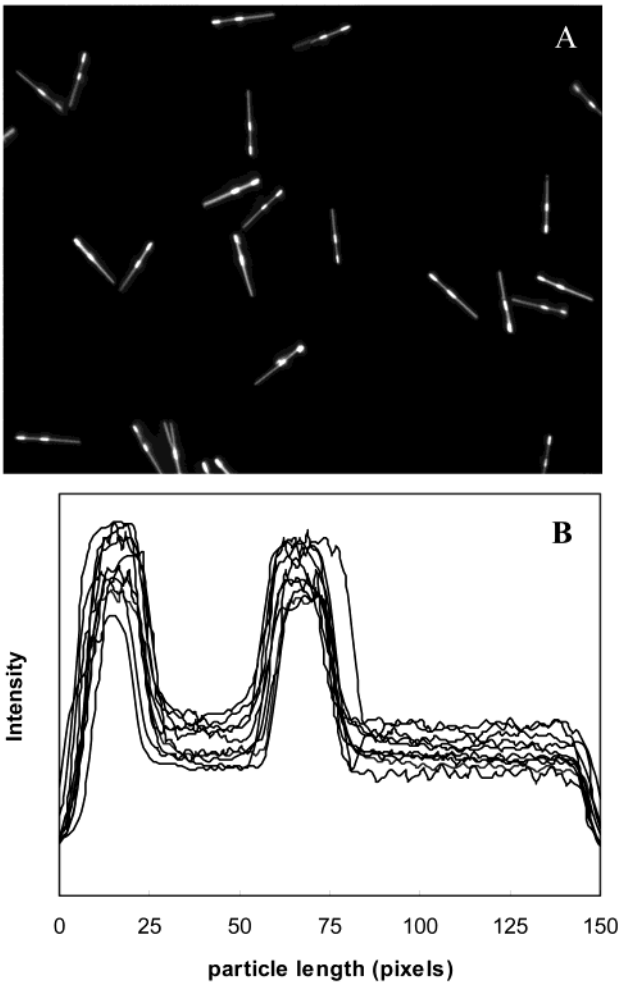

Figure 3. (A) Optical image of particles with stripe pattern 00001001 collected with 405-nm illumination and 1.4 NA, 160× magnification. The CCD format is 1030 pixels by 1300 pixels and 6.7 μm square pixels. At this magnification, the image size is 43 μm by 54 μm. (B) Extracted line profiles from 10 particles in the image.

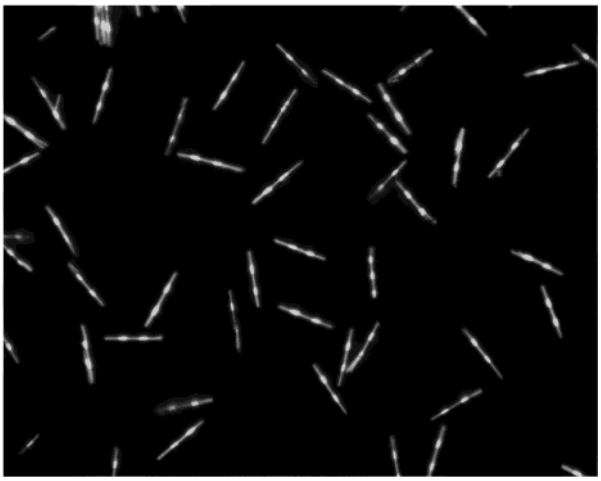

Figure 4. Typical image of stripe pattern 00100100. Image collected at 160× and 1.4 NA objective, illumination at 405 nm. At this magnification, the image size is 43 μm by 54 μm.

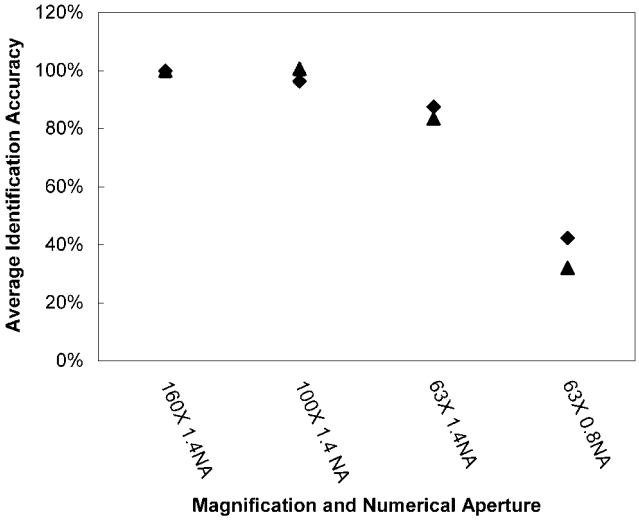

Figure 5. Relationship between the coherent transfer function and particle identification accuracy. (◆)Theoretical values for reduction in CTF at 2856 cycles/mm. (▲) Measured average reduction in identification accuracy with 160×, 1.4 NA scores normalized to 100%.

images would be detected by the program and identified with 100% accuracy. Toward that end, the computer program has a number of process settings that may be used to improve scoring accuracy. A discussion of the effect that all of these parameters has on particle identification is beyond the scope of this paper. Two particle properties that we use most often to improve scoring accuracy will be discussed, particle length and particle correlation coefficient. The software reports both of these properties for each particle found. The effect of using these properties as analysis gates can be illustrated by looking at striping pattern 00100100 (Figure 4). When 10 images containing these particles were analyzed, a total of 322 particles were found by the program, of which 210 were correctly identified for an unprocessed scoring accuracy of 65%. However, many of those particles that are incorrectly identified have low correlation coefficients. If a

Table 3. NBC Identification Accuracy[a]

ID	% correct	ID	% correct	ID	% correct	ID	% correct
00000001	98	00011100	96	00111011	96	01100110	99
00000010	98	00011101	79	00111100	96	01100111	94
00000011	99	00011110	94	00111101	86	01101101	88
00000100	97	00011111	98	00111110	97	01101110	96
00000101	97	00100001	99	00111111	95	01101111	82
00000110	97	00100010	97	01000001	97	01110001	92
00000111	94	00100011	96	01000010	95	01110011	50
00001000	99	00100100	98	01000011	91	01110111	96
00001001	96	00100101	79	01000101	97	01111001	81
00001010	98	00100110	98	01000110	95	01111011	57
00001011	96	00100111	99	01000111	94	01111101	80
00001100	88	00101001	90	01001001	83	01111110	98
00001101	97	00101010	96	01001010	95	01111111	46
00001110	98	00101011	97	01001011	93	10000001	63
00001111	100	00101100	99	01001101	86	10000011	82
00010001	96	00101101	100	01001110	95	10000101	97
00010010	96	00101110	97	01001111	92	10000111	79
00010011	99	00101111	95	01010001	96	10111101	34
00010100	99	00110001	96	01010011	92	11000011	54
00010101	99	00110010	98	01010101	74	11000111	87
00010110	95	00110011	93	01011010	86	11001111	42
00010111	94	00110101	94	01011110	98	11011011	71
00011000	98	00110110	97	01011111	70	11011111	54
00011001	92	00110111	99	01100001	94	11100111	29
00011010	98	00111001	74	01100011	99	11101111	75
00011011	98	00111010	95				

[a] For each striping pattern, 10 or more images were analyzed. The percent correct (identification accuracy) was determined by adjusting length and correlation coefficient gates such that accuracy was weighted 5× more heavily than the percent of particles used (see text for more detailed discussion).

minimum correlation of 0.75 is applied, 49 particles are discarded and 200/273 are correctly identified (73%). Raising the minimum correlation coefficient to 0.85 brings the scoring accuracy to 90%, leaving only 172 particles in the analysis. Discarding particles with large length variations can also improve scoring accuracy. For this batch, the average length was 135.5 pixels and the standard deviation 8.8 (5.7 ± 0.5 μm). If we do not use the correlation coefficient gate but instead discard those particles below 120 pixels and above 150, 71% are correctly identified (205/288). By filtering the raw results using both length and correlation coefficients, high scoring accuracy is easily obtained. In this process, we discard some correctly identified particles (increase false negative results) in order to remove incorrectly identified particles (decrease false positive results). The amount of particles that must be discarded is a function of the quality of the synthesis.

Limits Dictated by Optical Resolution. Optical imaging systems impose a low-pass filter on the spatial information that is available at the surface of striped particles. The result of this loss of high spatial frequency information is that distinctions between individual stripes become blurred. This limit to optical resolution is often discussed in terms of the Rayleigh criterion or Rayleigh limit. In our case, it is more useful to think in terms of the incoherent contrast-transfer function (CTF)[38] for the optical system rather than simply a limiting value. The incoherent contrast-transfer function measures the loss of image contrast that occurs when the image passes through a given optical element, objective, filter, CCD camera, etc. Clearly, if enough image contrast is lost, Au and Ag stripes will be impossible to distinguish. Maximum contrast is maintained when the highest numerical aperture, 100×, 1.4 NA objective, with an extra 1.6× of magnification is used. Because of pixelation, the additional 1.6× magnifier effectively improves the CTF of the CCD camera.

The data in Figure 5 reflect the effect of CTF on score accuracy. We collected images of 12 different striping patterns, using different magnifications and apertures, from 160× at 1.4 NA to 63× at 0.8 NA. For each stripe pattern the identification accuracy was normalized to 100% for the 160×, 1.4 NA combination. At each subsequent magnification−NA combination, the percent decrease in identification accuracy was calculated for each striping pattern and averaged. As can be seen the average relative identification accuracy declines systematically to below 40% at 0.8 NA and 63×.

For comparison, we calculated the CTF for the complete optical system, including objective[38] and camera[39] for a number of spatial frequencies. The result for the frequency 28.6×10^5 cycles/m appears in Figure 5. This frequency is 4× the fundamental spatial frequency of our striping patterns,[40] and the reduction in CTF is strongly correlated to our measured reduction in scoring accuracy. The fact that high spatial frequency information is needed to obtain the most accurate particle identification makes sense because it is the high-frequency information that helps sharpen the boundaries between stripes.

In addition to fundamental limitations set by optics, identification error is introduced when the particles do not lay flat on the

(38) Goodman, J. W. *Introduction to Fourier Optics*; McGraw-Hill: New York, 1988.

(39) Holst, G. C. CCD *Arrays Cameras and Displays*, 2nd ed.; SPIE: Bellingham, WA, 1998.

(40) Our segment length is 0.7 μm, giving a period of 1.4 μm. This results in a spatial frequency of $10^6/1.4$ or 7.1×10^5 cycles/m. The plotted CTF was calculated for a spatial frequency of 28.6×10^5 cycles/mm.

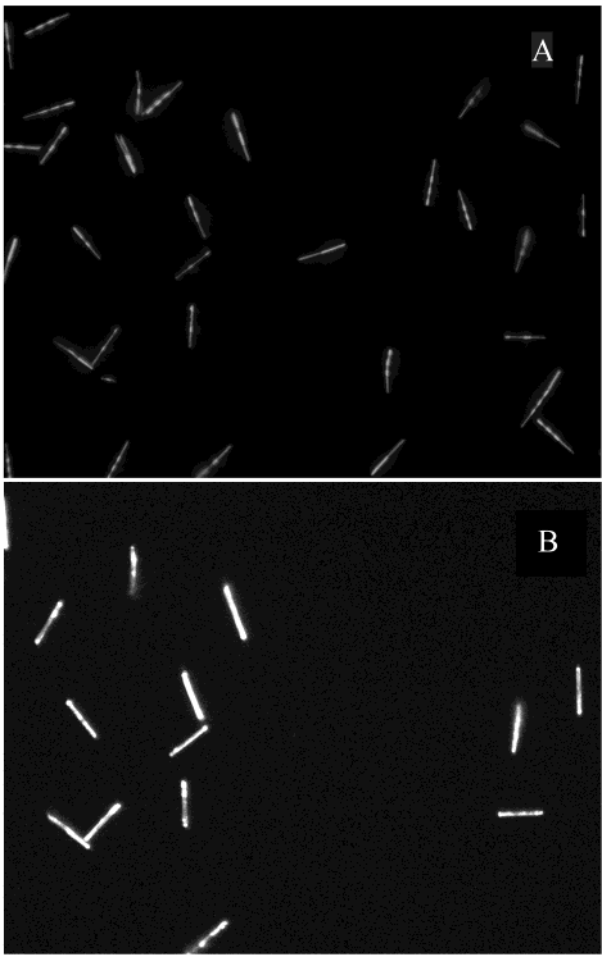

Figure 6. Reflectance and fluorescence image of mixed sample of particles. (A) Reflectance image showing particles with stripe patterns 00001111, 00010001, 00010101, 00010111, and 00011011. (B) Fluorescence image with particles having 00010001, 00010111, and 00011011 striping patterns showing fluorescence. Both reflectance and fluorescence images were collected at 100× overall magnification. Thus, the size of the image is 69 μm by 87 μm.

surface of the microwell tray. If one end of a particle is out of focus, that end will produce a less intense signal. This can often cause a single Ag stripe to be identified as Au.

NBC Library Generation. To better understand the problems that might be encountered when trying to accurately identify a large variety of particles, we began the synthesis of a 134-flavor library,[41] of which 102 have now been made. The target particle length was 6 μm. A consistent set of analysis parameters were applied as good compromise settings that would give us relatively low false positive rates without making the false negative rates too high. Only particles with lengths between 100 and 250 pixels (4.2−10.5 μm) were measured. Using these settings, our current ability to generate and identify a wide variety of striping patterns is illustrated by Table 3. As was mentioned earlier, it is almost always possible to obtain 100% accuracy if one is willing to ignore large numbers of particles. To generate Table 3, we optimized the combination of accuracy and percent used, with accuracy weighted 5× more heavily than percent used. The exception to this was that there was a minimum of 100 particles used for any striping pattern. Within these parameters, length gates and correlation coefficients were adjusted to give optimized results. With this set of data, 74 NBC flavors identify at >90% accuracy, 11 additional flavors are above 80% accuracy, and 17 are less than 80% accuracy. While the true false negative rates (which would require hand counting of all images) have not been calculated for all of these flavors, the general principle holds that higher accuracy could be obtained for nearly all flavors by either increasing the minimum flavor correlation coefficient allowed or by narrowing the range of widths accepted.

The most common problem is the misidentification of an Ag stripe as an Au stripe. For example, this is seen with NBC01011111, which is called NBC01011110 18% of the time. It is also seen with isolated terminal Ag stripes such as NBC00111101, which is correctly identified 86% of the time and called NBC00111100 11% of the time. Also, the software occasionally misidentifies an NBC that has part of its body off the edge of the acquired image. There are at least two possible causes for incorrect identification of Ag, both of which have been noticed through careful study of the microscope images. In the first instance, and despite the presence of the Au caps, during the removal of the Ag on the back of the alumina membrane, it is possible for HNO_3 to come into contact and etch Ag near the ends of the NBCs. This reduces the reflectivity of the Ag surface and in some cases can completely remove the terminal Ag. Second, if the end of the NBC containing the Ag stripe is not as well focused as the remainder of the rod, the signal will be diminished, leading to identification as Au. It should be noted that counterexamples of this phenomenon abound. Specifically, NBC01000001 can be correctly identified 97% of the time. While terminal Ag stripes are more vulnerable to damage, such damage does not always occur. We expect that as our control of the NBC synthesis and release process continues to improve, damage to terminal Ag sections of the particles will be greatly reduced. This will significantly increase the number of striping patterns for which high accuracy identification can be routinely obtained.

Fluorescence from Molecules Captured on Striped Particles. Figure 6 demonstrates that it is possible to use striped metallic particles as tools for chemical analysis. Figure 6A is the reflectance image from a set of particles with the striping patterns 00001111, 00010001, 00010101, 00010111, and 00011011. Three of these types of particles (00010001, 00010111, and 00011011) were coated with NeutrAvidin so that they would capture fluorescently tagged biotin. The others were uncoated and used as a control. As can be seen from the fluorescence image (Figure 6B), only those particles that were properly prepared to capture the fluorescent molecule are visible. By preparing each set of particles with unique surface chemistry, multiple fluorescence analyses may be carried out simultaneously. Applications of these particles to genomic analysis and immunoassays will be discussed in detail in a separate report.

CONCLUSION

It is useful to compare the barcoded metal particle approach to particle identification with the more widely used fluorescence bead approach for high levels of multiplexing. For fluorescence-based particle identification, the number of uniquely identifiable

(41) A maximum of 136 flavors may be made by using a two-metal, eight-stripe model. The all-Au (00000000) and all-Ag (11111111) are not included in the library because the current analysis program cannot distinguish between the two.

particles is determined by the number of discrete emission intensity levels that can be generated with a single dye and the spectral overlap of the two or more dyes present in a bead. For a single dye, the dynamic range of emission intensity is limited on the lower end by detection sensitivity and on the upper end by dye loading. The number of distinguishable levels between the high and low are determined by the precision of dye loading and the precision of the fluorescence measurements. To increase the total number of uniquely identifiable particles, either the number of distinguishable intensity levels must increase or the number of distinguishable dyes must increase. As additional dyes are used for particle encoding, the spectral overlap of the dyes (both emission and excitation bands) must be taken into account. This is likely to cause problems, particularly when one dye is at very high concentrations while a dye with a spectrally close emission feature is present in small amounts. In those cases, the emission tails from the dye at high concentration will begin to interfere with the emission of the dye at low concentration. The additional fluorescence dyes used to quantify binding of analytes will also complicate the picture. Each additional dye requires an added channel for detection, and each new intensity level requires improved precision in dye loading, fluorescence detection, or both.

For striped particles made with two metals, each additional stripe increases the number of uniquely identifiable particles by a factor of ~2 without changing the identification instrumentation. Correct identification is limited by the variability of stripe length (somewhat equivalent to dye-loading precision) and the total number of stripes that can be produced in a particle of reasonable length. Reasonable length may well be defined by other aspects of the desired assay rather than by particle identification parameters. Adding a third or fourth metal is philosophically equivalent to adding additional dyes to fluorescent beads, although it has somewhat different results. To add an additional metal requires the ability to accurately distinguish an additional reflectivity level, instead of an additional fluorescence emission band. This may be accomplished by increased precision in measurement or by measuring reflectivity at a different wavelength, which is somewhat similar to increasing the number of fluorescence data channels in the fluorescence measurement.

We are currently addressing many of the challenges with NBC identification that have been described above. A variety of plating solutions as well as plating conditions are being studied in order to find the set of experimental conditions that give the most reproducible stripe lengths. New identification algorithms are also being implemented that promise to improve our ability to distinguish between NBCs with very similar barcode patterns. To reduce problems caused by etching of Ag, it may be possible to replace the Ag that is currently used for the initial electrode with a more easily oxidized metal. This will allow us to remove that metal with a weaker oxidizing agent and therefore avoid etching of Ag in the NBC.

It is important to note that it is not necessary for all of the flavors in an NBC library to be successfully identified. As can be seen in Table 1, it is theoretically possible to make 3321 different striping patterns using the three-metal, eight-stripe model. If as little as one-third of those NBCs can be unambiguously identified, that leaves more than 1000 identifiable species. Currently, beads encoded with fluorescent dyes are available in 100 different varieties.[12]

Finally, we ultimately want to measure as many NBCs simultaneously as possible. One way to increase the number of particles measured is to decrease the magnification such that more particles are collected in a single image. As discussed above, decreasing the magnification puts more demands on the precision of synthesis and software capabilities but should be possible with the expected improvements in those two areas.

ACKNOWLEDGMENT

This work was partially funded by the National Institute of Standards and Technology, Grant 70NANB1H3028, and the National Institutes of Health−NIDDK, Grant 1R43DK059077-01. Special thanks go to Lou Dietz and Howard Schulman for their helpful comments on the manuscript.

Received for review February 4, 2002. Accepted March 25, 2002.

AC020073W